VERA User's Meeting 2019年12月13-14日 水沢VLBI観測所 岩手

Revealing evolutional relation of Miras and OH/IR stars based on VLBI astrometry

Akiharu NAKAGWA Kagoshima University

In a long term VLBI monitoring project of the Galactic Mira variables (Miras), we have determined annual parallaxes of dozen of Miras to a high degree of accuracy (better than 10%). From the measurements, we derived a period-Mk relation of the Galactic Miras as $MK = -3.52 \log P + 1.09 \pm 0.14$ (Nakagawa et al. 2016). Recently, we found that some Miras are not so bright as expected from the relation. This may indicate that characteristics of Miras are different between in the Galaxy and LMC.

Now, we started 43GHz VLBI observations of OH/IR stars, particularly toward the sources showing its pulsation period longer than 500 days. Miras are though to become OH/IR stars as they evolve. By comparing properties of circumstellar matters in Miras and OH/IR stars revealed by VLBI imaging, we want to confirm its evolutional relation.

We compiled astrometric measurements form VLBI and Gaia DR2 for ~40 long period variables. We think that VLBI gives better parallax estimation than Gaia when its distance is further than 190 pc.

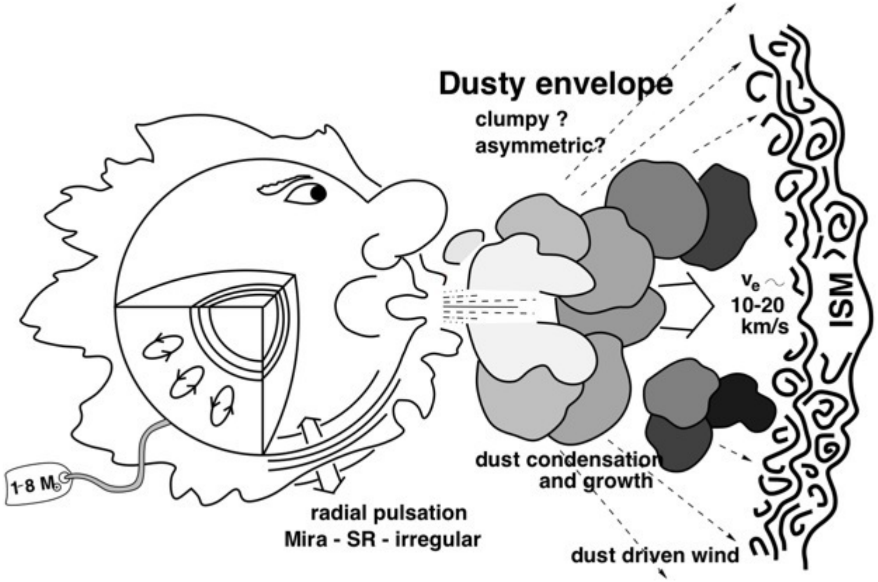

https://www.cfa.harvard.edu/~mmarengo/me/agb.html

LPVs
- Initial Mass : 0.8－8 M◎
- Period : 100－1000 d
- Mass loss→ Chemical evolution
- P-L relation → Usage of distance estimator

In the compilation of 65 project sources, we have measured parallaxes for ~30 sources using VERA (red colored sources). Recently, we started new observation of OH/IR stars to compare characteristics between Miras and OH/IR stars.

ID	Src.	Type	R.A.	Dec.
1	W Hya	SR	13h49m01.9980s	-28d22m03.488
2	T Lep	Mira	05h04m50.7999s	-21d54m16.500
3	RX_Boo	SR	14h24m11.5998s	+25d42m13.000
4	S_Crt	SR	11h52m45.1000s	-07d35m48.100
5	AP Lyn	Mira	06h34m33.8999s	+60d56m26.199
6	R UMa	Mira	10h44m38.3999s	+68d46m32.298
7	WX_Psc	Mira	01h06m25.8998s	+12d35m53.000
8	Z Pup	Mira	07h32m38.1000s	-20d39m29.199
9	SY Scl	Mira	00h07m36.2000s	-25d29m40.000
10	Y Lib	Mira	15h11m41.2999s	-06d00m41.399
11	VX UMa	Mira	10h55m39.8999s	+71d52m09.800
12	GX Mon	Mira	06h52m46.8999s	+08d25m19.000
13	U Lyn	Mira	06h40m46.5000s	+59d52m01.600
14	T UMa	Mira	12h36m23.5000s	+59d29m13.000
15	S CrB	Mira	15h21m24.0000s	+31d22m02.600
16	SW Lib	Mira	15h55m33.3999s	-12d51m05.099
17	FS Lib	Mira	16h00m23.8000s	-12d20m57.500
18	IRC-20540	Mira	19h08m56.0000s	-22d14m19.399
19	IRC+10374	Mira	18h43m36.7000s	+13d57m22.800
20	X Hya	Mira	09h35m30.3000s	-14d41m28.600
21	R Cnc	Mira	08h16m33.7999s	+11d43m34.500
22	FV_Boo	SR	15h08m25.8000s	+09d36m18.199
23	RU_Ari	SR	02h44m45.5000s	+12d19m03.000
24	RW_Lep	SR	05h38m52.7000s	-14d02m27.199
25	BW_Cam	Mira	05h19m52.5600s	+63d15m55.798
26	BX_Cam	Mira	05h46m44.2999s	+69d58m24.199
27	U_Ori	Mira	05h55m49.2000s	+20d10m30.699
28	QX_Pup	Mira	07h42m16.8298s	-14d42m52.100
29	RS_Vir	Mira	14h27m16.3998s	+04d40m41.100
30	SY_Aql	Mira	20h07m05.4000s	+12d57m06.299
31	SV_Peg	SRb	22h05m42.0850s	+35d20m54.536
32	R_Tau	Mira	04h28m18.0000s	+10d09m44.798
33	OZ_Gem	Mira	07h33m57.7500s	+30d30m37.798
34	V353_Pup	SR	07h46m34.1510s	-32d18m16.260
35	HU_Pup	SR	07h55m40.1600s	-28d38m54.840
36	HS_UMa	LPV	11h35m30.70408s	+34d52m04.1775
37	R_LMi	Mira	09h45m34.28304s	+34d30m42.7839
38	BX_Eri	SR	04h40m32.754s	-14d12m02.39
39	V637_Per	SR	03h54m02.28s	+36d32m17.6
40	U_CVn	Mira	12h47m19.61s	+38d22m30.5
41	RU_Hya	Mira	14h11m34.39861s	-28d53m07.4089
42	NSV17351	OHIR	07h07m49.38s	-10d44m05.9
43	R_Peg	Mira	23h06m39.16689s	+10d32m36.0892
44	R_Hya	Mira	13h29m42.78187s	-23d16m52.7747
45	OH127.8	OHIR	01h33 51.21s	+62d26m53.2
46	NSV25875	OHIR	22h19m27.48s	+59d51m21.7
47	UU_Peg	Mira	21h31m04.156s	+11d09m13.24 92
48	R_Cas	Mira	23h58m24.87336s	+51d23m19.7011
49	S_Ser	Mira	15h21m39.53475s	+14d18m53.1002
50	W_Leo	Mira	10h53m37.43245s	+13d42m54.3666
51	OH32.8-0.3	OHIR	18h52m24.682333s	-00d14m57.612
52	V391CYG	Mira	19h40m52.394300s	+48d47m41.52658
53	RAFGL5201	OHIR	06h34m28.052569s	-05d03m42.85697
54	OH83.4-0.9	OHIR	20h50m58.619647s	+42d48m11.44793
55	OH141.7+3.5	OHIR	03h33m30.618480s	+60d20m08.85024
56	CU_Cep	OHIR	22h11m31.882483s	+57d02'17.46857"
57	DU_Pup	Mira	07h35m03.978770s	-23d59'14.80023"
58	RAFGL2445	OHIR	19h44m07.000754s	+35d14'08.25184"
59	OH39.7+1.5	OHIR	18h58m30.094784s	+06d42'57.69806"
60	EUAND	C	23h19m58.881502s	+47d14'34.57638"
61	AWTAU	Mira	05h47m30.209209s	+27d08'12.40939"
62	I17411-3154	Mira	17h44m24.003874s	-31d55'35.42862"
63	OH26.5+0.6	OHIR	18h37m32.51s	-05d23'59.2"
64	OH42.3-0.1	OHIR	19h09m07.466221s	+08d16'22.70258"
65	TXCAM	Mira	05h00m51.156996s	+56d10'54.09311"

Period-Mk diagram of the Galactic Miras. In conversions from mk to Mk, we use distances determined from VERA observation. In the shaded area, we found some Miras which represent smaller Mk magnitude than those expected from the known P-Mk relation. In a study by Urago et al.(in prep), they try to explain reasons of this effect.

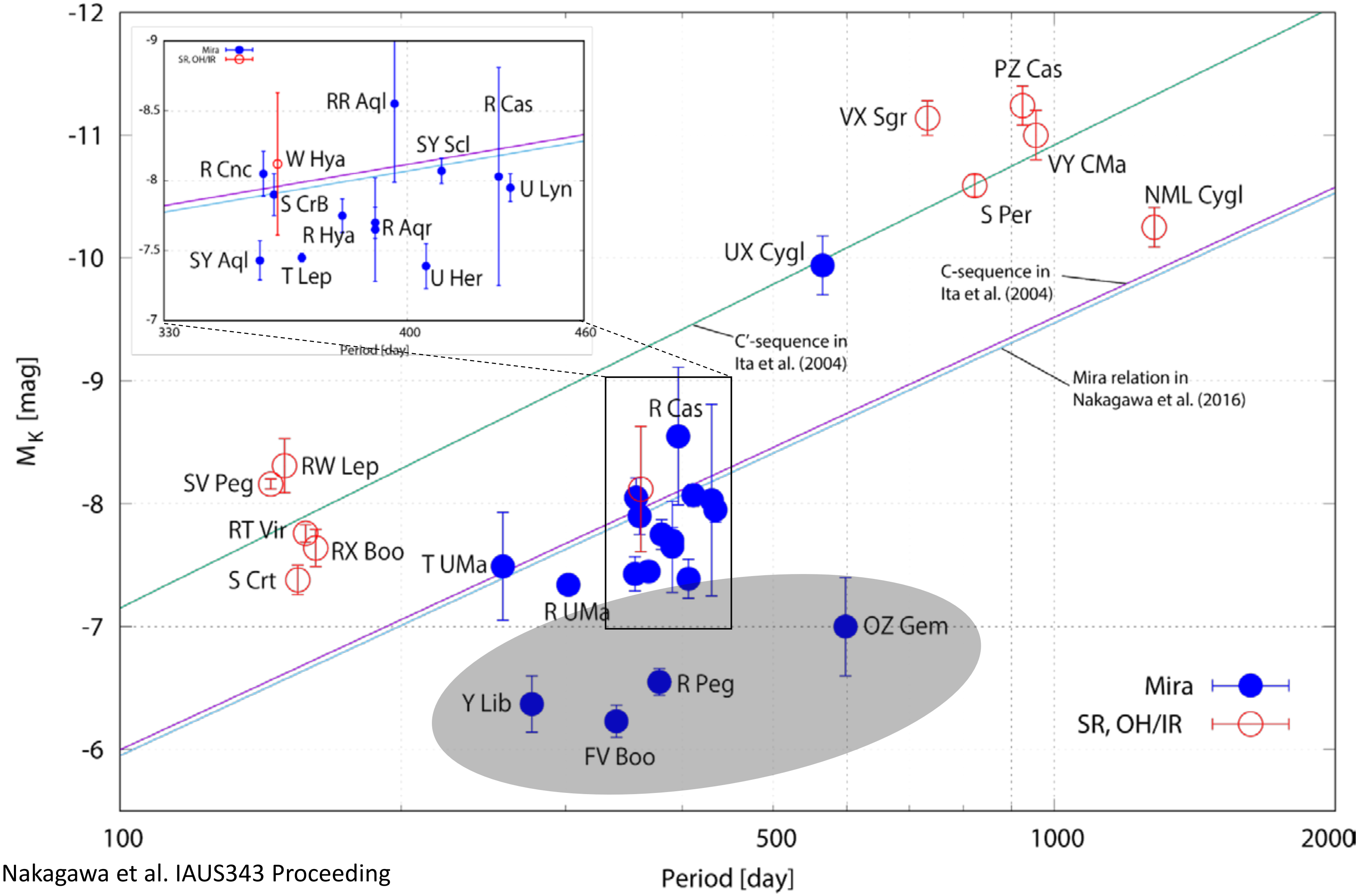

Nakagawa et al. IAUS343 Proceeding

Observations of LPVs to study evolution from Miras to OH/IR stars

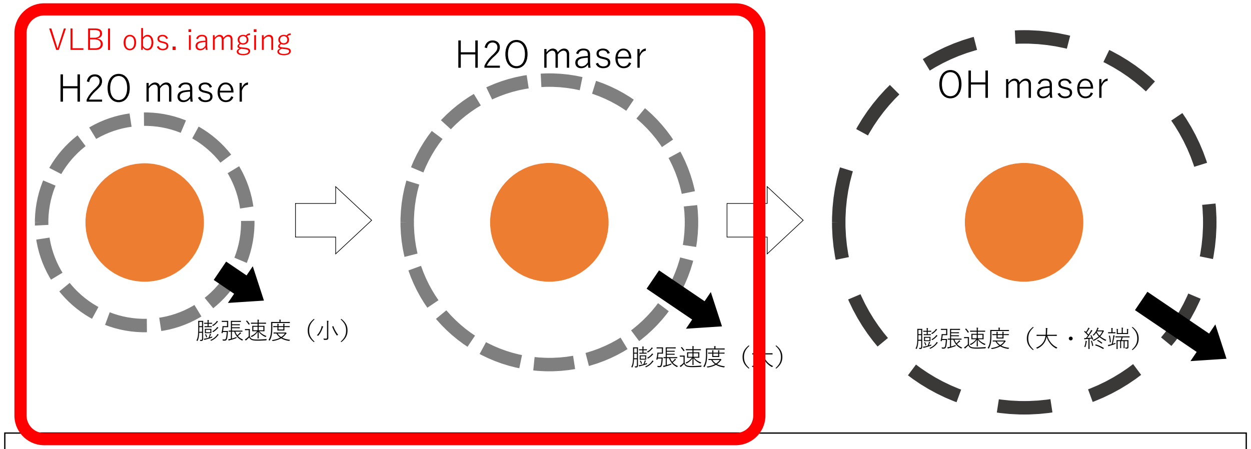

To understand evolution from Miras to OH/IR stars, we want to reveal,

>distribution of circumstellar maser
>spectral shape of H2O, SiO, and OH masers
>SED from NIR to FIR.

進化	① Mira型変光星 ⇨	② Mira型変光星 ⇒ OH/IR星 ⇨	③ OH/IR星
メーザーの種類	星周でH2Oメーザーが励起される ⇨	H2Oメーザーが加速を受けて外層へと広がる ⇨	H2Oメーザーが外縁部で光乖離されてOHメーザーが励起され始める
メーザーの速度	ある速度で膨張 ⇨	次第に加速されて速度は速くなる ⇨	加速が終わり、速度は終端速度に達する
メーザーのスペクトル	H2Oメーザー 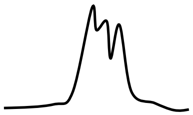 膨張速度を反映したスペクトルの広がり。 ⇨ Single dish obs. (H2O)	H2Oメーザー 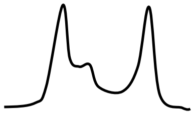 加速により幅が徐々に広がる様子が見える。 ⇨	OHメーザー 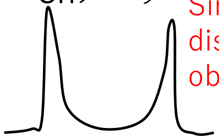 加速が終わり終端速度に到達したOHメーザーが観測される。切り立つエッジが特徴的。 Single dish obs. (OH)
SEDの様子	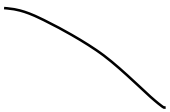 可視から赤外まで広く輻射あり	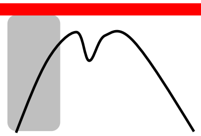 ダストにより可視が抑えられ再放射による赤外の過多 IR spectroscopy	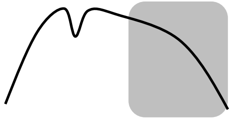 厚いダストによる中間赤外から遠赤外の過多が目立つ

VLBI observation of extreme-OH/IR stars

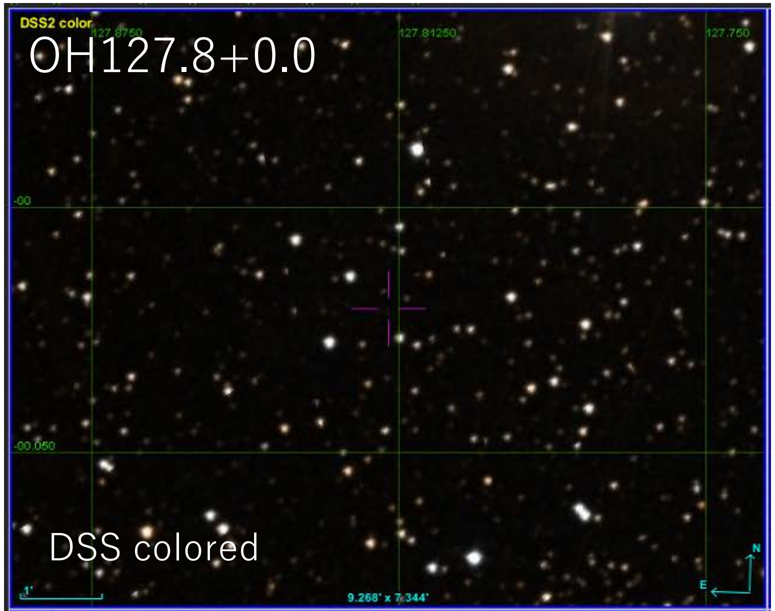
DSS2 color
OH127.8+0.0
127.8750
127.81250
127.750
-00
-00.050
DSS colored
1'
9.268' x 7.344'
N
E

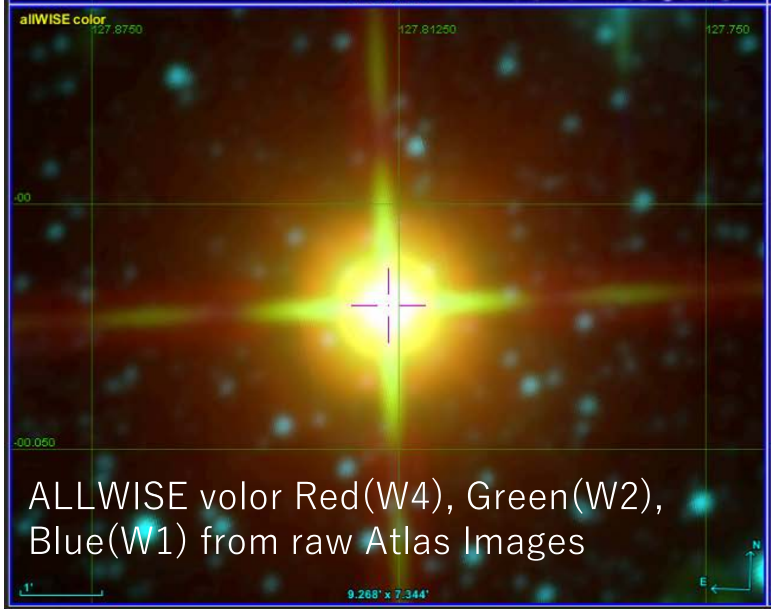
allWISE color
127.8750
127.81250
127.750
-00
-00.050
ALLWISE volor Red(W4), Green(W2), Blue(W1) from raw Atlas Images
1'
9.268' x 7.344'
N
E

In parallax measurements of deeply enshrouded sources, VLBI can be a powerful tool. We started VLBI observations of an extreme-OH/IR star NSV25875 using the VERA at 43GHz.

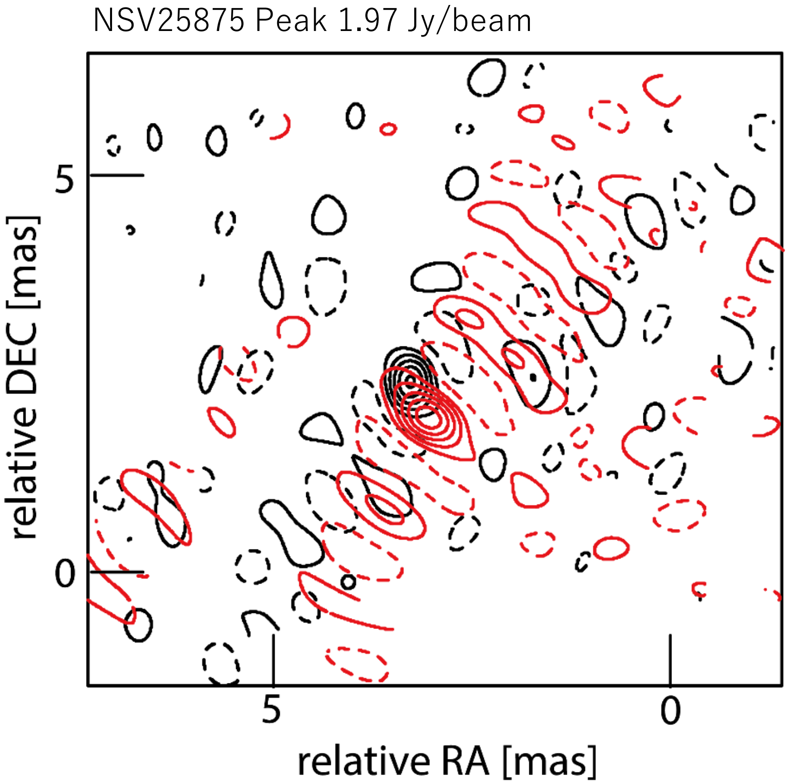

- 43GHz astrometric observation with VERA from Nov. 2017
- QSO: J2231+5922, ~240mJy@43GHz
- SiO maser (v=2), S/N=10

Phase referencing observation @43GHz, 2Gbps (512MHz BW for QSO)

NSV25875

Parallax = 0.38 ± 0.13 mas, D = 2.60 ± 0.85 kpc

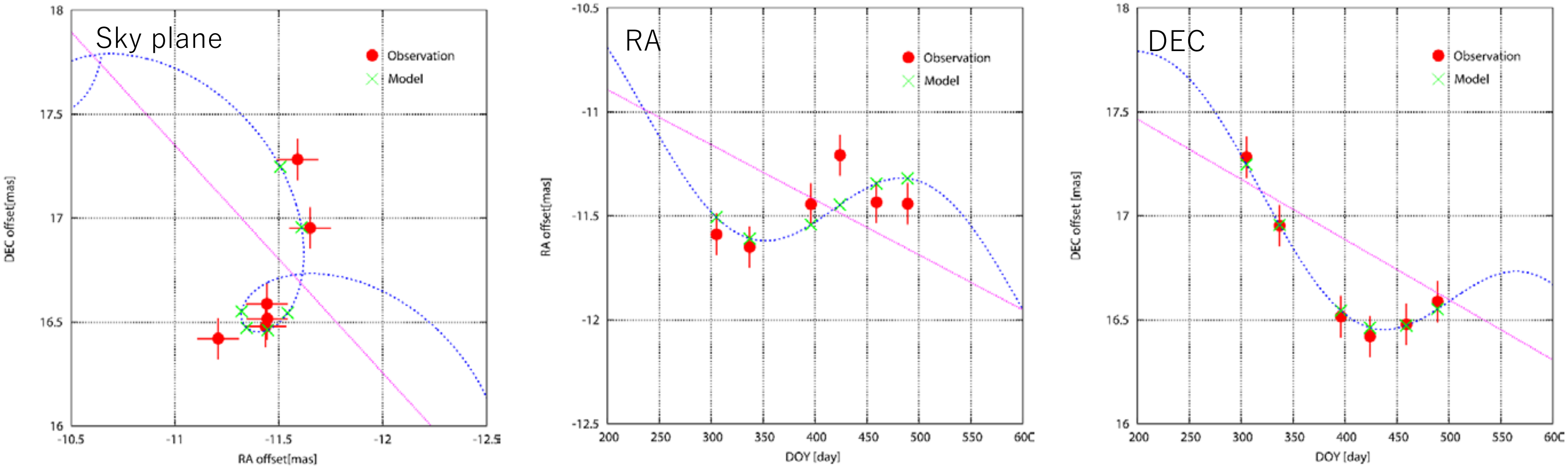

OH127.8+0.0

Parallax = 0.22 ± 0.08 mas, D = 4.54 ± 1.14 kpc

(μx, μy) = (−1.18 ± 0.12, −1.10 ± 0.11) [mas/yr]

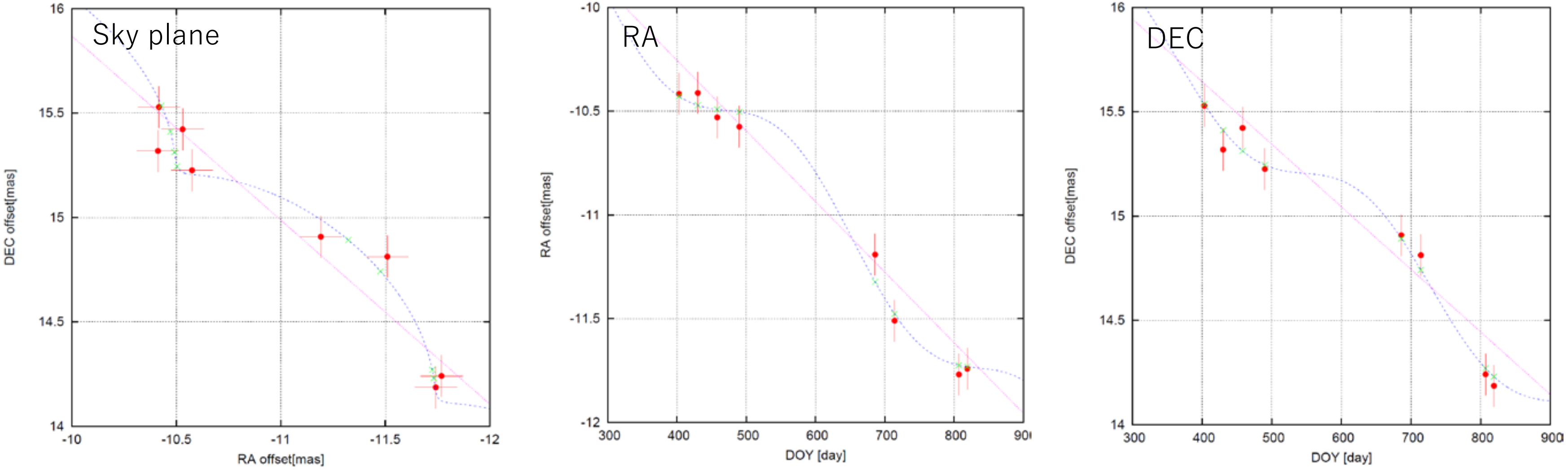

Acceleration of H2O maser in NSV17351

From 45 years data in literature, we found acceleration of H2O maser in NSV17351.

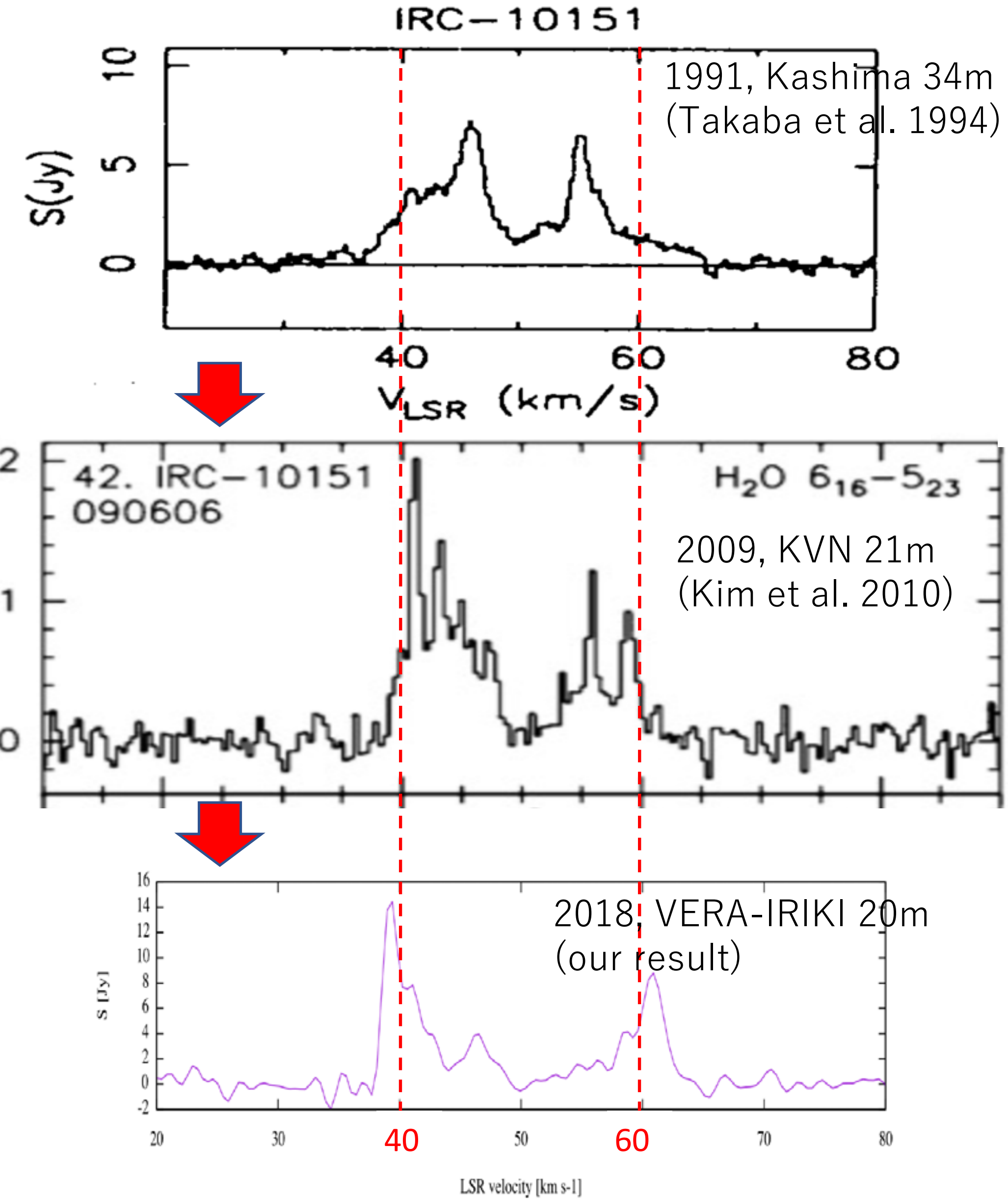

1991, Kashima 34m
(Takaba et al. 1994)

2009, KVN 21m
(Kim et al. 2010)

2018, VERA-IRIKI 20m
(our result)

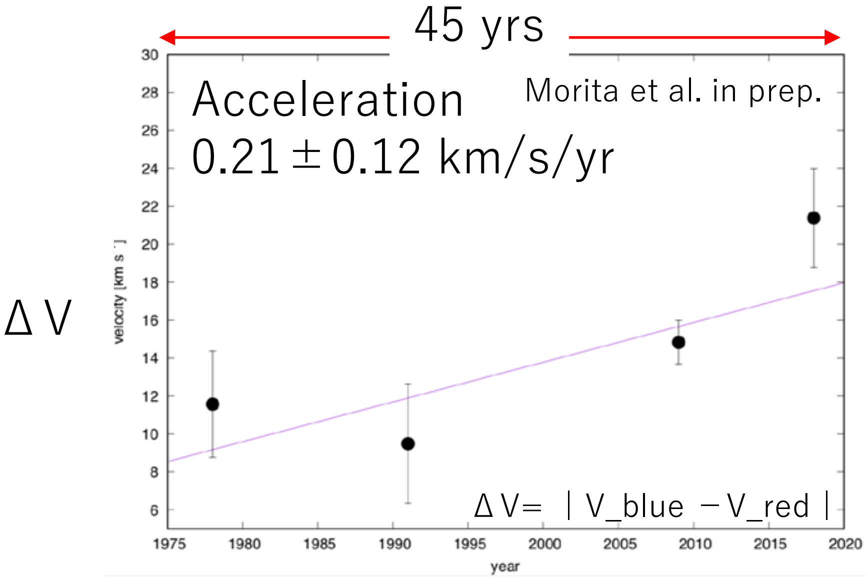

45 yrs

Acceleration
0.21 ± 0.12 km/s/yr

Morita et al. in prep.

ΔV= | V_blue − V_red |

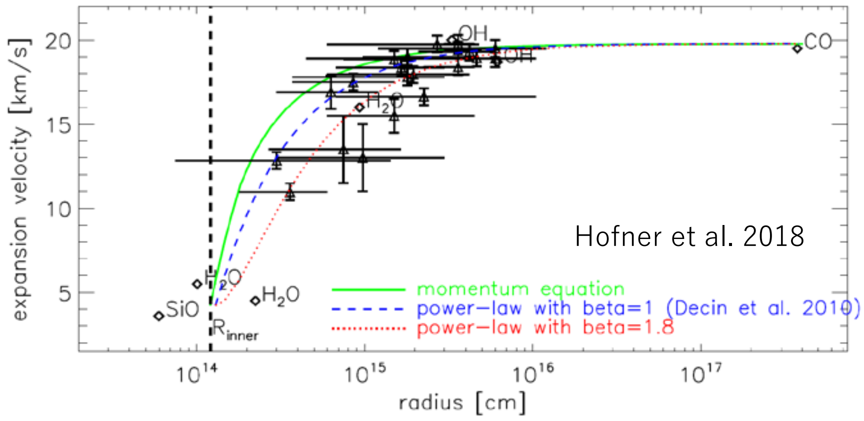

Hofner et al. 2018

Fig. 8 The velocity profile of the M-type star IK Tau. It illustrates the different techniques used to determine the radial dependence of the gas expansion velocity (see text for details). The diamonds show the places in the CSE where the SiO, H_2O, and OH masers are located, and the terminal expansion velocity obtained from the CO($J = 1-0$) line. The triangles show the places in the envelope that contribute the most to the H_2O line emissions observed with the Herschel Space Observatory. The horizontal bars show the minimum and maximum radial distance of the line emission regions. The vertical bars show the uncertainty on the observed line widths. The expansion velocities obtained from solving a momentum equation (full green line), and from a power law, Eq. (9), with $\beta = 1$ (blue dashed line) and 1.8 (red dotted line) are shown. Image reproduced with permission from Decin et al. (2010), copyright by ESO

Similarity of spectrums, H2O and OH maser

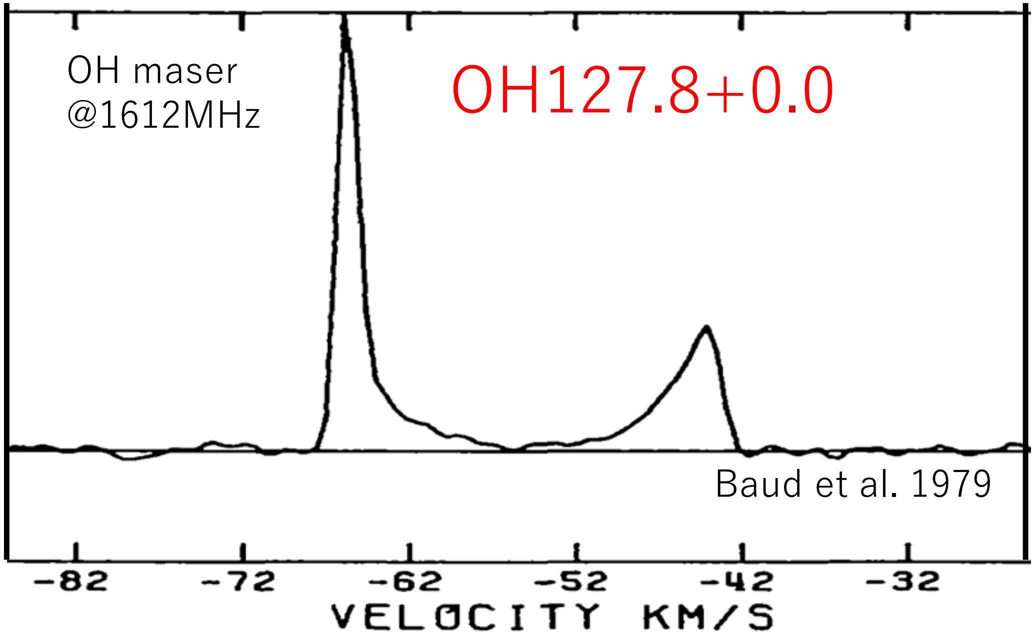

Baud et al. 1979

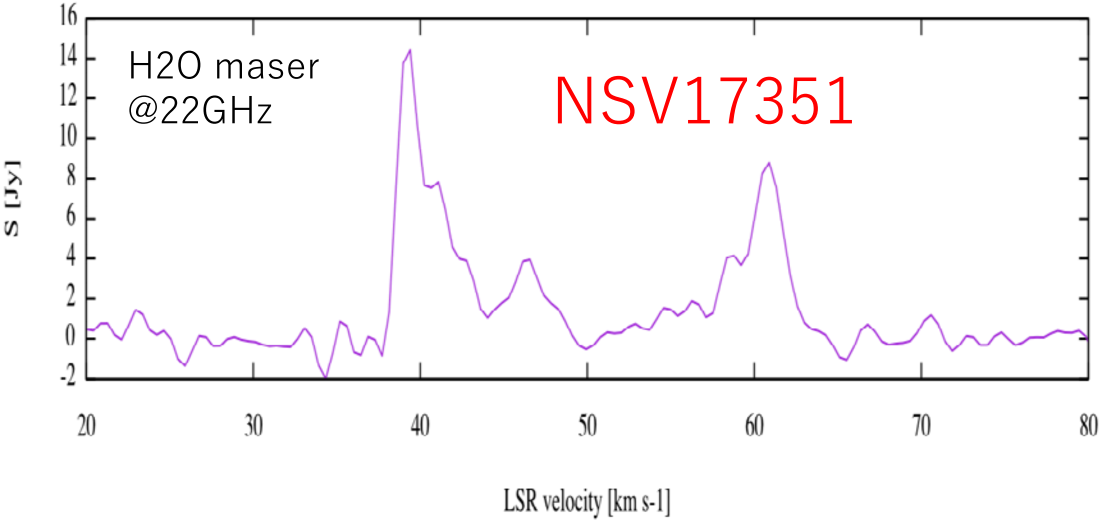

Similar characteristics between H2O and OH

- Steep edges
- U-shaped hollow

<Hypothesis>
H2O gas in NSV17351 has experienced an acceleration and reached a terminal velocity in the last 45 years.

H2O shell radius at the terminal velocity is calculated to be >65 au.

Morita et al. in prep.

Similarity of positions between H2O and OH maser also supports the hypothesis

Bluest emission was found at an assumed stellar position.

OH maser @ 1612 MHz

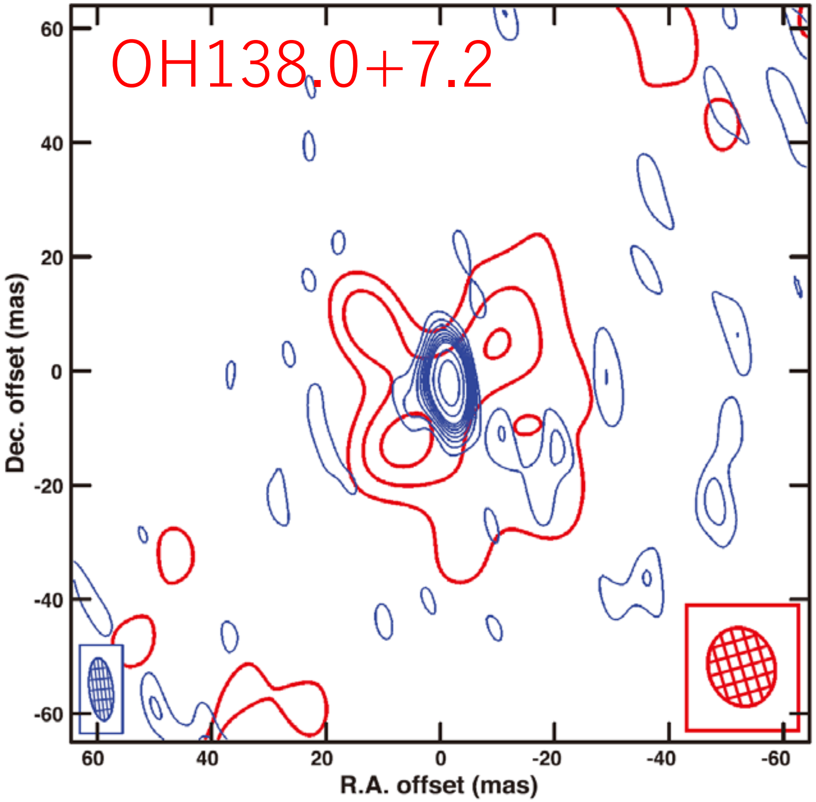

Orosz et al. 2018

H2O maser @ 22 GHz

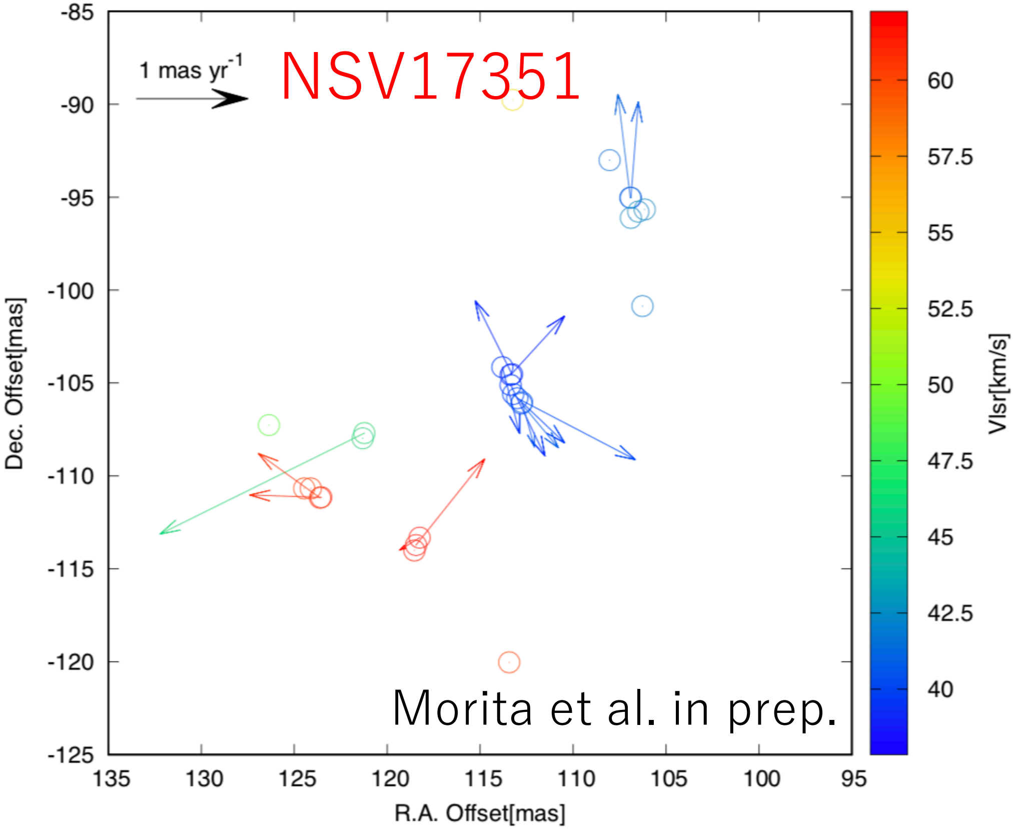

Our result

...However, sky plane motion of the bluest masers are puzzling.

Distances of three Extreme-OH/IR stars

Methods:

- VLBI Parallax (< 10%)
- Gaia DR2 parallax (invisible or weak, diffuse)
- Phase-lag method (20% accuracy)
- Kinematic distance (factor of 2, Reid et al. 1991)

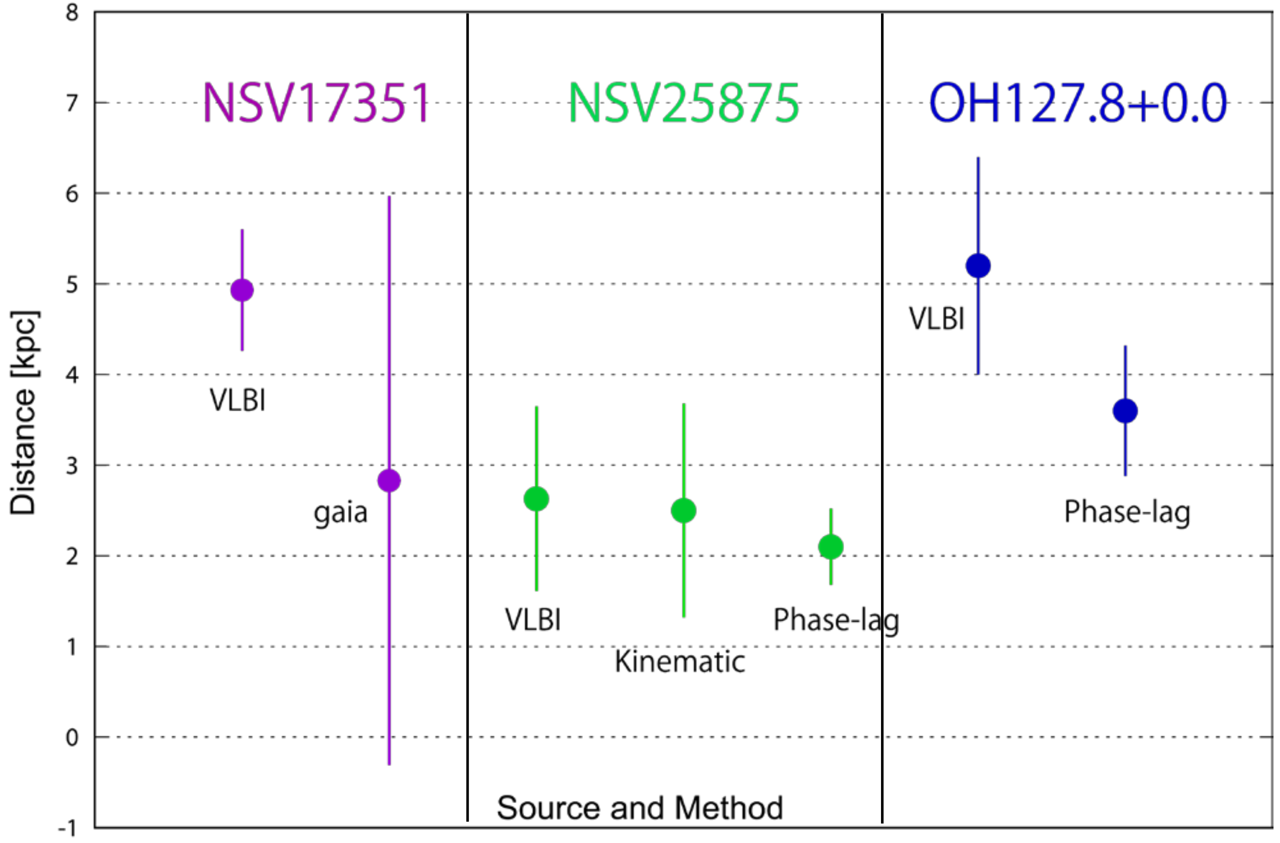

Phase-lag distances from Engels et al. 2015

VLBI and Gaia : Parallax

To evaluate difference of parallax measurements from VBLI and Gaia, we introduced a parameter Γ. From the histogram, we could not find clear systematic difference between VLBI and Gaia.

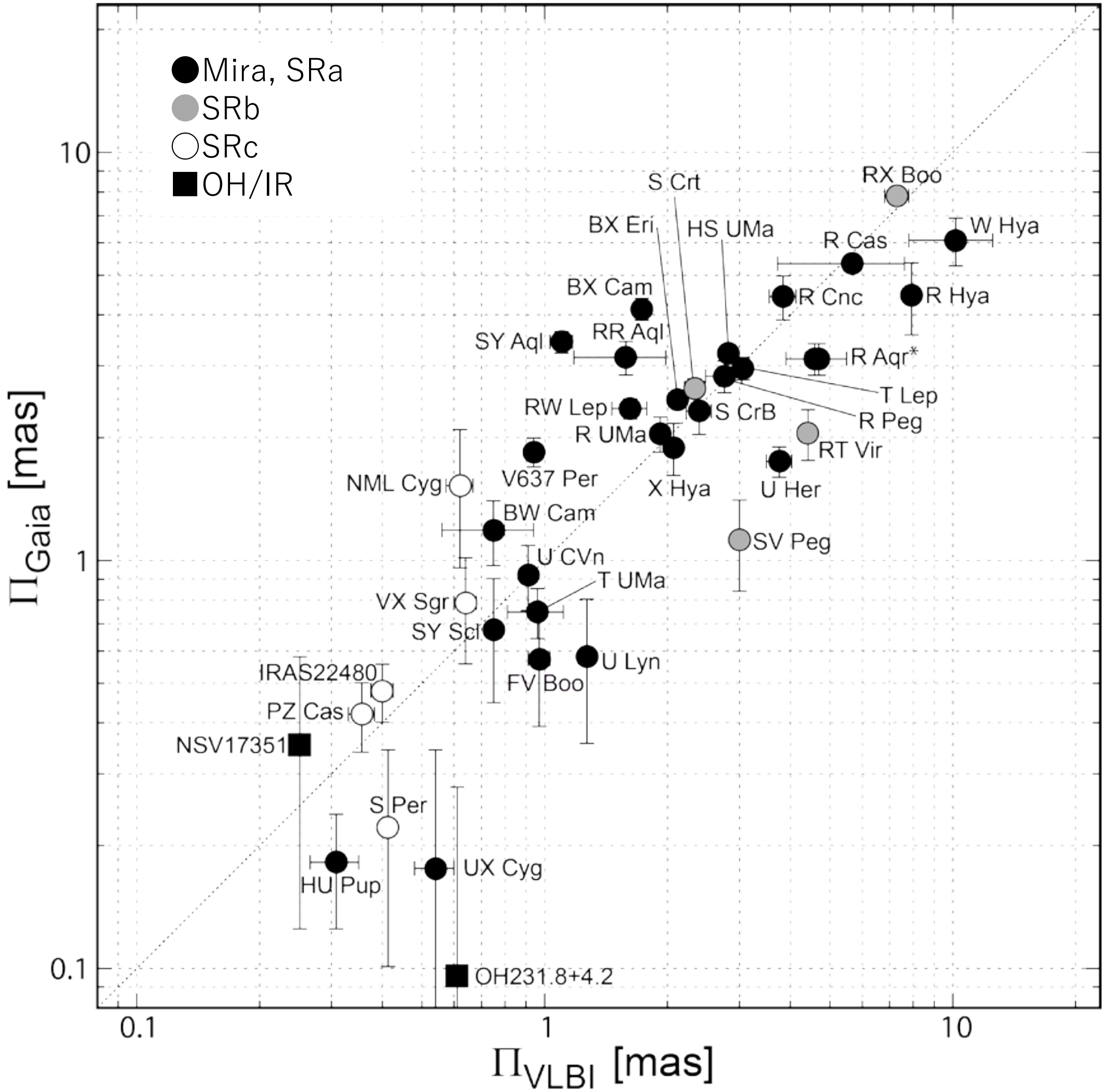

We define a parameter for comparison,

$$\Gamma = \frac{\Pi_{\mathrm{VLBI}} - \Pi_{\mathrm{Gaia}}}{\sqrt{\sigma^2_{\Pi_{\mathrm{VLBI}}} + \sigma^2_{\Pi_{\mathrm{Gaia}}}}}$$

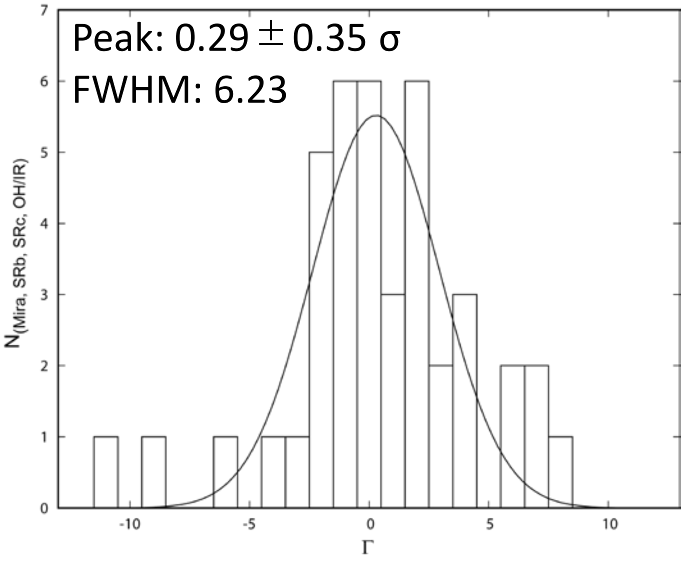

Nakagawa et al. in prep.

VLBI and Gaia : Parallax vs error

In the right figure, parallaxes and its formal errors are presented. Filled and open circles indicate measurements from VLBI and Gaia, respectively. From linear fitting, we obtained two lines and presented them with two types of lines. They cross at Π=5.20 mas (corresponding distance = 192pc). In observation of parallax smaller than 5.20 mas, VLBI is more useful than Gaia.

VLBI ———

$y=(0.96\pm0.13)\mathrm{Log}\Pi-1.20\pm0.06$

Gaia ··········

$y=(0.29\pm0.07)\mathrm{Log}\Pi-0.72\pm0.04$

D>190 pc : VLBI is more reliable
D<190 pc : Gaia is more reliable

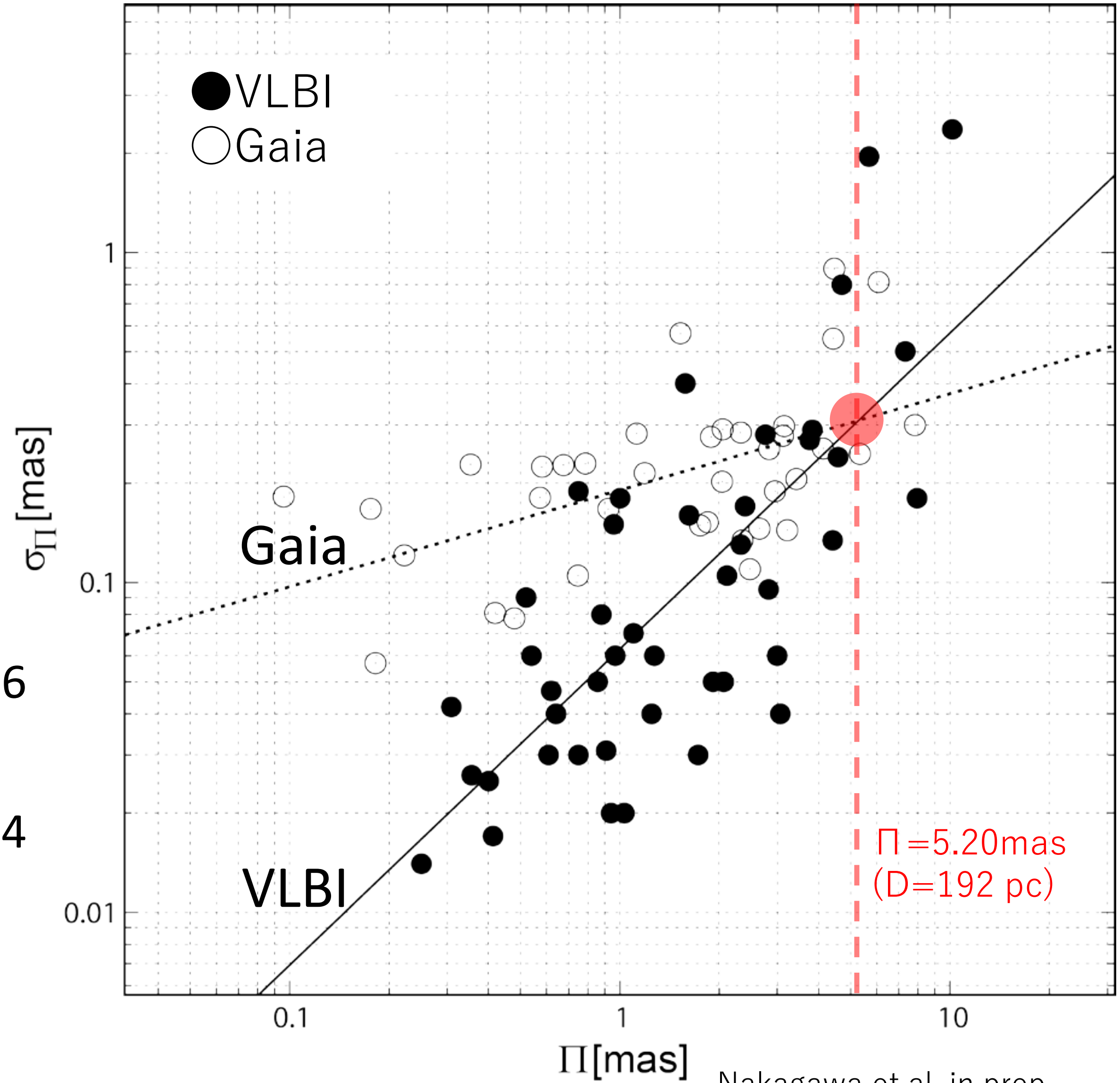

Nakagawa et al. in prep.

VLBI and Gaia : Comparison of proper motion

Difference of systemic angular motions and corresponding velocities are presented. In angular motion plane, differences of large part of the sources fall within 5mas/yr. We converted the angular motion to velocities using parallaxes from VLBI, then presented the velocity difference in right panel. Large part of the source fall within velocity range of ±15km/s. This velocity scale is almost same as that of outflow velocity of circumstellar matters in long period variables.

(Δμx, Δμy) [mas/yr]

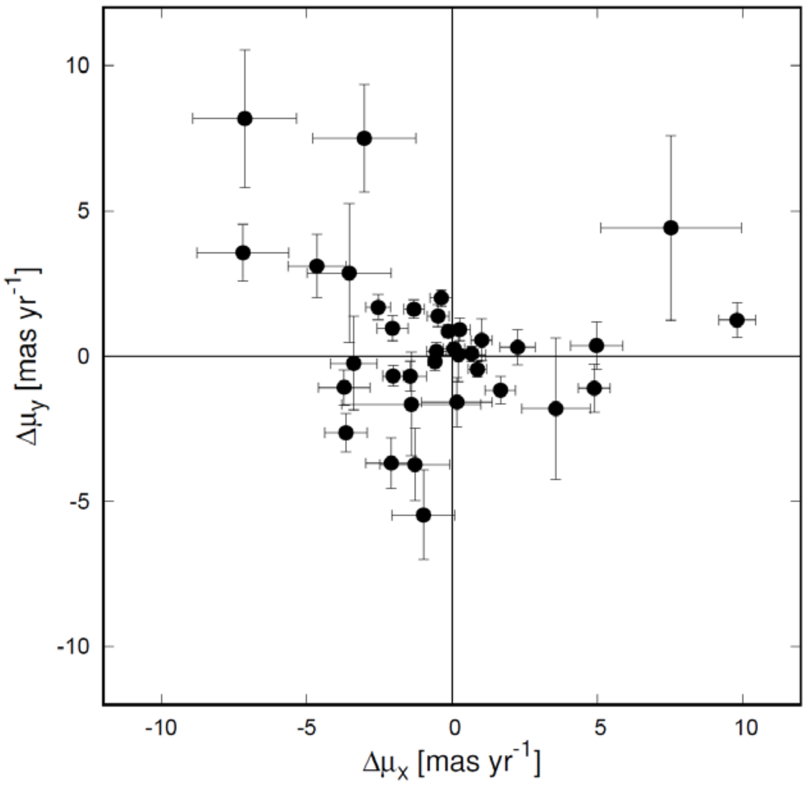

(ΔVx, ΔVy) [km/s]

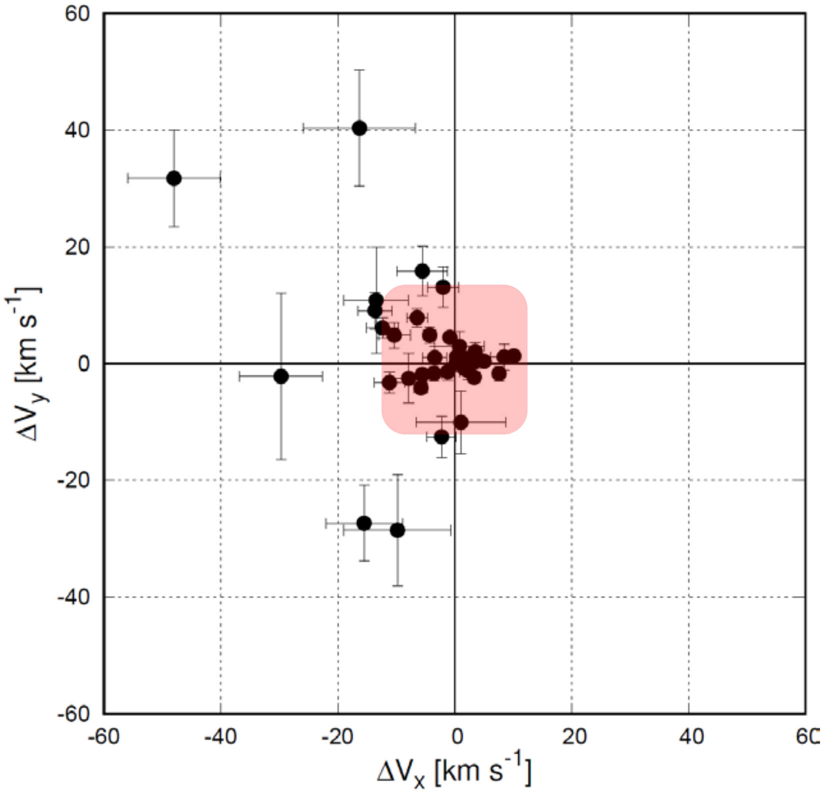

Nakagawa et al. in prep.